Available online at www.sciencedirect.com
SCIENCE DIRECT
Polymer 47 (2006) 2455–2459
polymer
www.elsevier.com/locate/polymer

Epitaxial crystallization of poly(butylene adipate) on highly oriented isotactic polypropylene thin film

Yinjie Sun [a], Huihui Li [a,d], Yun Huang [b], Erqiang Chen [b], Zhihua Gan [c], Shouke Yan [a,*]

[a] State Key Laboratory of Polymer Physics and Chemistry, Institute of Chemistry, The Chinese Academy of Sciences, Beijing 100080, People's Republic of China
[b] Department of Polymer Science, School of Chemistry, Peking University, Beijing, People's Republic of China
[c] CAS Key Laboratory of Plastic Engineering, Institute of Chemistry, The Chinese Academy of Sciences, Beijing 100080, People's Republic of China
[d] Graduate School of the Chinese Academy of Sciences, Beijing, 100039, People's Republic of China

Received 25 August 2005; received in revised form 5 February 2006; accepted 8 February 2006
Available online 28 February 2006

Abstract

The crystallization behaviors of PBA on highly oriented *i*PP substrate both from solution and isotropic melt were studied by means of optical microscopy, AFM, X-ray and electron diffractions. The results clearly indicate the occurrence of heteroepitaxy of PBA on the *i*PP substrate in its β-form with both molecular chains $\pm 50°$ apart from. This is based on the existence of perfect matching between the interchain distance of β-PBA along [100] direction and the distance of the out-sticking methyl side group arrays along the [101] direction of the (010) *i*PP plane. Electron diffraction pattern further confirms that the (010) lattice plane of the β-PBA is in contact with the *i*PP substrate.

Keywords: Poly(butylene adipate); Polypropylene; Epitaxy

1. Introduction

Owing to the soft matter characters, more and more polymeric materials have been used in many fields. This leads to extensive studies on every aspect of polymeric materials. Among many others, biodegradable polymer materials have attracted great interests due to their environmental and ecological advantages in the recent two decades [1,2]. For biodegradable polymeric materials, biodegradation is one of the most important properties for practical application. The biodegradation rate is, on the other hand, another very important parameter for specific applications. Therefore, effort has been made in attempts to modulate the biodegradation rate of biodegradable polymers. It is well known that the biodegradation rate of a polymer depends not only on its chemical structure but also on its morphology such as crystallinity, molecular chain packing and crystal surface. Abe et al. reported that the degradation rate of semicrystalline polyesters is inversely proportional to their lamellar thickness [3]. The dependence of degradation rate on crystal size makes it possible to adjust the degradation rate of semicrystalline polyesters simply through regulating its processing condition. This is, however, not sufficient enough since most of the polyesters exhibit polymorphs, which also affect the degradation rate. For example, poly(butylene adipate) (PBA), a semicrystalline polyester, exhibits two different modifications designated as α and β [4–7]. Experimental results on enzymatic degradation of melt-crystallized, α- and β-PBA films revealed that the α-PBA degraded relatively faster than its β-counterpart, even though the α-crystals have larger crystal size than the β-crystals [8]. Therefore, successful domination of the crystalline structure while regulating the crystal size during thermal process is of great importance.

Epitaxial crystallization, defined as the oriented overgrowth of a crystalline phase on the surface of a substrate (host crystal) [9,10], is widely employed for controlling the crystalline structure and orientation of a wide variety of crystallizable materials [11–18]. For example, Lotz et al. have once successfully modulated different crystalline structures of several polymers through regulating the crystalline structure of the used substrates [16,17]. Lovinger has then skillfully controlled the crystallization of poly(vinylidene fluoride) from melt into its piezoelectric and pyroelectric β-form at atmospheric pressure through epitaxy [18]. Taking those into account, epitaxial crystallization can, undoubtedly, find potential application in dominating the crystalline structure of biodegradable polyesters during different thermal processes

* Corresponding author. Tel./fax: +86 10 82618476.
E-mail address: skyan@iccas.ac.cn (S. Yan).

0032-3861/$ - see front matter © 2006 Elsevier Ltd. All rights reserved.
doi:10.1016/j.polymer.2006.02.002

for regulating their crystal sizes. There are, however, only few reports on the epitaxial crystallization of PBA on inorganic substrates [20,21].

In our previous study, we found that the PBA can be fixed in β-form via epitaxy on highly oriented PE substrate at any crystallization conditions [22]. The purpose of this paper is to present some experimental results regarding the epitaxial behavior of PBA on highly oriented polypropylene (*i*PP) substrate.

2. Experimental

The PBA used in this work was produced by BASF AG Ludwigshafen, Germany. The weight-average molecular weight of PBA is about 4×10^4, with a polydispersity of 1.7. Its melting temperature is measured to be 57 °C. Before sample preparation, the PBA was purified by precipitating from its chloroform solution. Commercial grade isotactic polypropylene (*i*PP) (GB-2401) produced by Yanshan Petroleum and Chemical Corp., China, with melt flow index of 2.5 g/10 min, $M_w=4.4\times10^5$, and melting temperature of 170 °C, was used in present work.

Uniaxially oriented ultrathin *i*PP films were prepared according to a melt-draw technique introduced by Petermann and Gohil [19]. According to this method, a small amount of a 0.5 wt% solution of the *i*PP in xylene was poured and uniformly spread on a preheated glass plate where the solvent was allowed to evaporate at the preparation temperature (ca. 135 °C). After evaporation of the solvent, the *i*PP thin molten layer (about 1 μm in thickness) was then drawn up by a motor driven cylinder with a drawing speed of about 2 cm/s. The obtained films (30–50 nm thick) can be directly used for transmission electron microscopy (TEM) observations [23,24].

Composite double layers of PBA/*i*PP were prepared by dipping the glass slides partially covered by highly oriented *i*PP thin films into 2 or 0.1 wt% PBA chloroform solution. The PBA layers on the backsides (without *i*PP substrate) of the glass slides were removed after evaporation of the chloroform. Thick films prepared by dipping the *i*PP film into 2 wt% PBA chloroform solution, ca. 10 μm, were used directly for POM observation and X-ray measurement. Thin films prepared by dipping the *i*PP film into 0.1 wt% PBA chloroform solution were first floated onto the surface of distilled water and then transferred onto 400 mesh TEM copper grids or fresh cleaved mica surface for TEM or atomic force microscopy (AFM) observations, respectively. For melt crystallization, the above as prepared samples were heat-treated at 75 °C (far above the melting point of PBA) for 10 min to erase possible effects of the thermal history and subsequently cooled at a rate of 30 °C/min to (a) 35, (b) 30, and (c) 25 °C for isothermal crystallization.

For AFM observation, a NanoScope III scanning microscope (Digital Instruments) was used. The experiment was carried out in the tapping mode. A JEM GEOL-100CX electron microscope operated at 100 kV and an OLYMPUS BH-2 optical microscope were used for TEM and optical microscopy observation, respectively. The optical micrograph shown in this paper was taken under polarized light.

Wide-angle X-ray diffraction (WAXD) experiments were carried out using a 12 kW rotating-anode generator (Cu Kr) in combination with a Geigerflex D/max-RB diffractomter. The reflection peak positions and widths were calibrated with silicon powder ($2\theta>15°$) and silver behenate ($2\theta<10°$). Powder patterns were taken in reflection mode at a scan rate of 10°/min within the 2θ angle region of 15–30°.

3. Results

An optical micrograph of the as prepared PBA/*i*PP double layers is shown in Fig. 1. For a direct comparison, a boundary region was chosen with the thin *i*PP film located at the right side of the picture. The boundary line of *i*PP substrate can be easily recognized in Fig. 1. The molecular chain direction of the *i*PP substrate, as indicated by an arrow, is parallel to the boundary line. Since the *i*PP film is too thin to provide birefringence contribution at present condition, the picture directly illustrates the effect of *i*PP substrate on the crystallization PBA. One can see that crystallization of PBA on highly oriented *i*PP substrate from solution (right part of Fig. 1) yields a quite different morphology as compared with that on glass slide (left part of Fig. 1). The PBA crystallized on glass slide produces irregular spherulitic structure without preferential orientation. This is the common morphology of polymer crystallized from solution on glass slide. In contrast, on the *i*PP substrate, the nucleation density is largely enhanced and no individual PBA spherulites can be identified. On the boundary, transcrystalline zone of PBA induced by *i*PP can be clearly seen. These imply that the *i*PP substrate displays active nucleation ability toward PBA. To clarify the crystalline structure of PBA crystallized on glass and *i*PP substrates, wide angle X-ray diffraction measurement is conducted. Fig. 2 presents the X-ray diffraction patterns of PBA solution grown on neat glass side as well as *i*PP substrate. Here, the *i*PP substrate film is too thin to be detected by X-ray diffractometer. The diffraction peaks are assigned as the (110) and (020) reflections of PBA crystal in its β-modification, reflecting the crystallization of PBA from solution in β-form regardless of the substrate. The intensity difference of the diffraction peaks

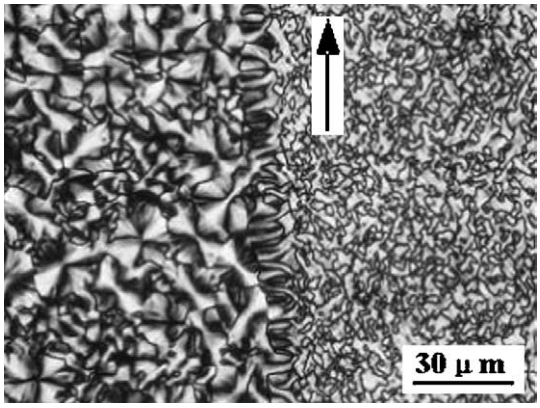

Fig. 1. A POM micrograph shows the morphologies of PBA crystallized on a boundary region of *i*PP substrate from solution. The *i*PP substrate is located in the right of the picture. The arrow indicates its molecular chain direction.

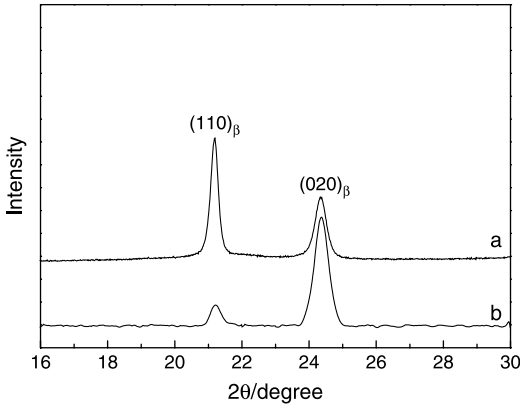

Fig. 2. WAXD patterns of PBA crystallized from solution on (a) glass substrates and (b) *i*PP surface.

of PBA crystallized on neat glass slide and *i*PP substrate indicates the existence of the preferred orientation of PBA on *i*PP substrate.

Detailed structural information of PBA crystallized on *i*PP surface from solution is revealed by AFM observation. Fig. 3 presents an AFM phase image of the PBA crystallized from solution on highly oriented *i*PP surface. The arrow in the picture represents the drawing direction of the *i*PP film during preparation. From Fig. 3, it can be clearly seen that a cross-hatched lamellar structure of PBA arises with the molecular chains predominantly ca. 50° apart from the chain direction of *i*PP substrate. This has close resemblance with the epitaxial crystallization of many other zigzag chain polymers on the highly oriented *i*PP substrate [25–27], and indicates the occurrence of heteroepitaxy of PBA on the *i*PP substrate. Fig. 4 shows the electron diffraction pattern of the epitaxial double layers and a sketch of it with the main reflections being indexed. The appearance of reflection spots of both PBA and *i*PP on the electron diffraction pattern (Fig. 4(a)), confirms that both PBA and *i*PP substrate layers exhibit high degree of orientation. All of the PBA reflection spots in Fig. 4(a) can be accounted for its orthorhombic unit cell in β-form. This further confirms that epitaxial crystallization of PBA from solution on *i*PP substrate is in its β-form. There exist two sets of PBA diffractions with chain axis in the film plane. The molecular

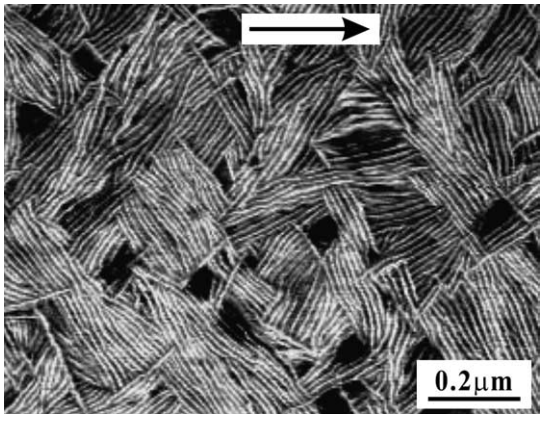

Fig. 3. An AFM phase image of PBA crystallized on the *i*PP substrate from solution. The arrow shows the chain direction of *i*PP substrate.

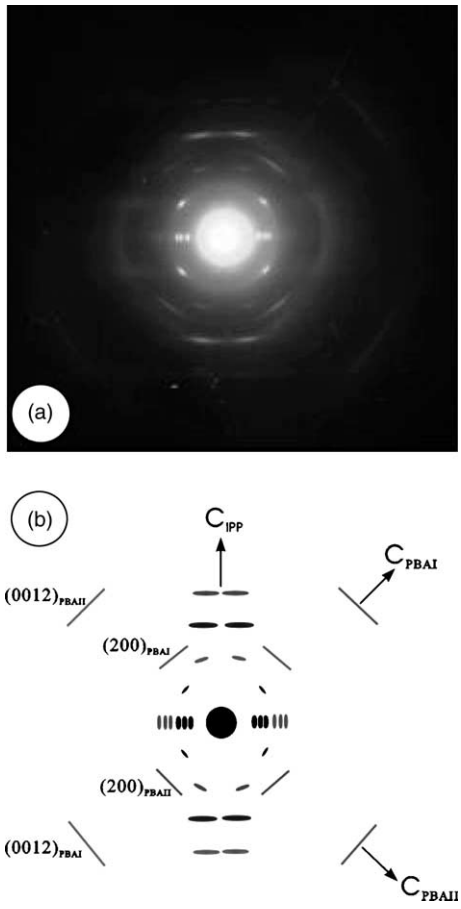

Fig. 4. (a) An electron diffraction pattern and (b) its sketch with main reflections being indexed of PBA/*i*PP double layers as shown in Fig. 3. The solid ellipses represent the electron diffractions of *i*PP, while the lines represent the reflection spots of PBA.

chains of PBA are inclined by ±50° from the molecular axis of the *i*PP substrate. This is in good agreement with the observed morphology shown in Fig. 3. Moreover, the absence of (020) PBA reflection and the appearance of strong (200) PBA reflection indicate that the *ac* plane of PBA, i.e. the (010) plane, is in contact with the *i*PP substrate.

Similar epitaxial structure was also observed for the melt crystallized PBA on *i*PP substrate at crystallization temperatures from 20 to 35 °C. Fig. 5(a)–(c) show the optical micrographs of PBA/*i*PP double layers, which were heat-treated at 75 °C for 10 min and subsequently cooled at a rate of 30 °C/min to (a) 35, (b) 30, and (c) 25 °C for isothermal crystallization. Boundary regions were used to reflect the exact same thermal conditions for the PBA crystallized on glass slides and *i*PP substrates. The *i*PP substrates are located at the lower right corners of the pictures. The chain directions of *i*PP substrates are parallel to the boundary lines as indicated by the arrows. It was reported that crystallizing the PBA at temperatures above 32 °C, results in the formation of relatively larger spherulites in its α form. When crystallizing the PBA at temperatures lower than 27 °C, except for the reduction of spherulite size, the PBA crystallizes into its β-form. The PBA crystallized in temperature range of 27–32 °C shows spherulites with banded structure composed of both α- and β-crystals [22,28]. From Fig. 5(a)–(c),

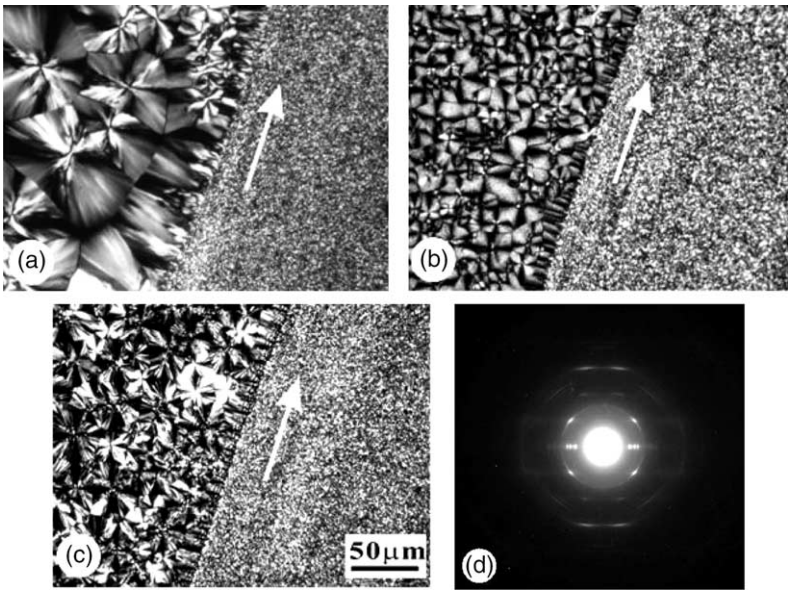

Fig. 5. Optical micrographs showing the morphologies of PBA crystallized from melt on *i*PP films and glass substrates. The crystallization temperatures were (a) 35, (b) 30, and (c) 25 °C. (d) their electron diffraction patterns. The arrows indicate the chain direction of *i*PP substrates.

evident changes can be identified for the PBA crystallized on the neat glass surface at different temperatures. This is in good accordance with the early reported results. On the contrary, no noticeable difference between the samples crystallized on *i*PP substrates at different temperatures could be recognized under optical microscope. Electron diffraction results (Fig. 5(d)) indicate that the PBA crystallizes epitaxially on the *i*PP substrate in its β-form at all used crystallization temperatures. This indicates that the *i*PP substrate exhibits also the structure controlling ability toward the PBA crystals.

4. Discussion

Since the early 1980s, heteroepitaxial crystallization of polymers onto various substrates has been an active subject in field of polymer science. Among many others, much attention has been paid to the systems of zigzag chain polymers with *i*PP [11,12,25,29–31], e.g. polyethene (PE) and *i*PP system, in which the chain axes of the two polymers oriented ca. 50° apart. As shown in Fig. 6, an understanding at the molecular level has been achieved on the parallel alignment of PE chains onto the oblique methyl group rows in the lateral *ac* plane of *i*PP with a 0.5 nm intermolecular distance for a chain-row matching [32]. For the present case, the PBA exhibits two different modifications designated as α and β [4–7]. In the β-form, the PBA chains exhibit planar zigzag conformations and pack in an orthorhombic unit cell with dimensions $a=0.506$ nm, $b=0.735$ nm, and $c=1.467$ nm. Its *ab* projection is almost identical to the crystalline structure of polyethylene. Therefore, a similar epitaxial crystallization of β-PBA on *i*PP as the PE/*i*PP system is expected. The only difference is that now a perfect matching (even better than *i*PP with PE) is found between the interchain distance of β-PBA along [100] direction (0.505 nm) and the distance of the methyl side group arrays along the [101] direction of the (010) *i*PP plane (0.505 nm). This leads to a change of contact plane from (100) for PE to (010) for PBA. On the other hand, in its α-crystals, the planar zigzag PBA chains are packed in a monoclinic unit cell with dimensions $a=0.67$ nm, $b=0.80$ nm $c=1.42$ nm, and $\beta=45.5°$. Comparing that with the monoclinic unit cell of *i*PP ($a=0.665$ nm, $b=2.096$ nm, $c=0.65$ nm and $\beta=99.2°$), excellent matching can also be found between the interchain distance of both α-PBA and *i*PP crystals along the [100] directions with a mismatching of 0.8%. One may argue that the epitaxial crystallization of α-PBA on the highly oriented *i*PP substrate is, however, not observed. To explain this phenomenon, detailed structure characters of *i*PP and PBA should be analyzed. Fig. 7(a) shows the *ac* projection of α-PBA. If we superimpose the PBA on *i*PP substrate with their *a*-axes parallel, the PBA chains will incline either 53.7° (Fig. 7(b)) or 35.3° (Fig. 7(c)) with respect to the chain direction of *i*PP. This means that the PBA chains cannot set in the arrays composed of out-sticking methyl groups

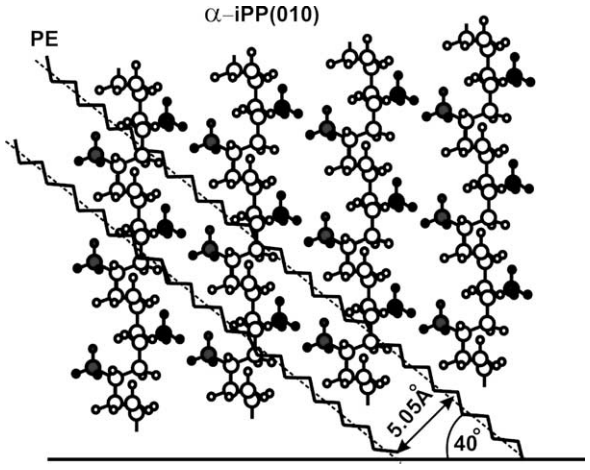

Fig. 6. A sketch shows the chain-row matching of the zigzag chain polymers on the (010) lattice plane of α-*i*PP.

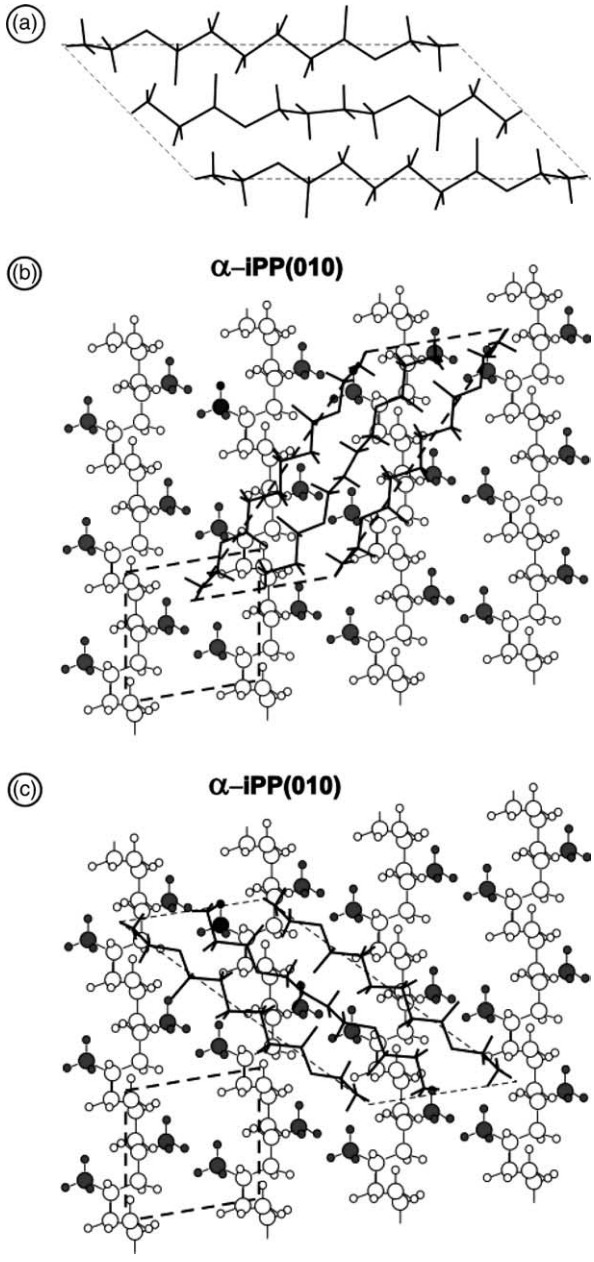

Fig. 7. An *ac* projection of the crystalline structure for α-PBA crystals and its possible alignments on (010) lattice plane of α-*i*PP with the *a*-axes of both polymers parallel.

of *i*PP. In other words, the PBA and *i*PP molecular chains cannot closely contact each other. This may enhance the interface free energy of the system and weaken the interaction between PBA and *i*PP. As a result, no epitaxial crystallization of α-PBA on highly oriented *i*PP substrate is observed.

5. Conclusions

The crystallization behaviors of PBA on highly oriented *i*PP substrate both from solution and isotropic melt were studied by means of optical microscopy, AFM, X-ray and electron diffractions. The results clearly indicate that the PBA can crystallize epitaxially on the oriented *i*PP substrate with its molecular chains $\pm 50^{\circ}$ apart from the chain direction of *i*PP substrate crystals. Owing to the perfect matching between the interchain distance of β-PBA along [100] direction (0.505 nm) and the distance of the out-sticking methyl side group arrays along the [101] direction of the (010) *i*PP plane (0.505 nm), the epitaxial crystallization of PBA on *i*PP substrate results in the formation of β-PBA crystals with its (010) lattice plane in contact with the *i*PP substrate. On the other hand, even though excellent matching can be found between the interchain distance of both α-PBA and *i*PP crystals along the [100] directions with a mismatching of 0.8%, due to the different β setting angles of PBA and *i*PP, an epitaxial crystallization of α-PBA crystals on highly oriented *i*PP substrate has not be realized. This provides us a useful way to control the crystalline modification of PBA during regulating its crystal size.

Acknowledgements

The financial support of the National Natural Science Foundation of China is gratefully acknowledged.

References

[1] Huang SJ. Encyclopedia of polymer science and engineering, vol. 2. New York: Wiley-Interscience; 1985 pp. 20.
[2] Fujimaki T. Polym Degrad Stab 1997;30:7403.
[3] Abe H, Doi Y, Aoki H, Akehata T. Macromolecules 1998;31:1791.
[4] Fuller CS, Erickson CL. J Am Chem Soc 1937;59:344.
[5] Fuller CS, Erickson CL. J Am Chem Soc 1939;61:2575.
[6] Fuller CS, Erickson CL. J Phys Chem 1939;43:323.
[7] Minke R, Blackwell J. J Mcromol Sci Phys 1979;B16:407.
[8] Gan Z, Kuwabara K, Abe H, Iwata T, Doi Y. Polym Degrad Stab 2005;87:191.
[9] Seifert H. Structure and properties of solid surfaces. Chicago: University of Chicago Press; 1953.
[10] Bonev I. Acta Crystallogr Sect A 1972;28:508.
[11] Wittmann JC, Lotz B. Prog Polym Sci 1990;15:909.
[12] Petermann J. Epitaxy on and with iPP. In: Karger-Kocsis J, editor. Polypropylene: structure, blends and composites. London: Chapman and Hall; 1995. p. 140.
[13] Zhang J, Yang D, Thiery A, Wittmann JC, Lotz B. Macromolecules 2001;34:6261.
[14] Wittmann JC, Lotz B. J Polym Sci, Polym Phys Ed 1981;19:1837.
[15] Wittmann JC, Lotz B. J Polym Sci, Polym Phys Ed 1981;19:1853.
[16] Kopp S, Wittmann JC, Lotz B. Polymer 1994;35:908.
[17] Kopp S, Wittmann JC, Lotz B. Polymer 1994;35:916.
[18] Lovinger AJ. Polymer 1981;22:412.
[19] Petermann J, Gohil RM. J Mater Sci 1979;14:2260.
[20] Pouget E, Almontassir A, Casas MT, Puiggali J. Macromolecules 2003;36:698.
[21] Minke R, Blackwell J. J Mcromol Sci Phys 1980;B18:233.
[22] Sun Y, Li H, Huang Y, Chen E, Zhao L, Gan Z, Yan S. Macromolecules 2005;38:2739.
[23] Yan S, Petermann J. Polymer 2000;41:6679.
[24] Yan S, Lieberwirth I, Katzenberg F, Petermann J. J Macromol Sci B Phys 2003;B42:641.
[25] Petermann J, Xu Y, Loos J, Yang D. Macromol Chem 1992;193:611.
[26] Tao X, Yan S, Yang D. Chin Chem Lett 1993;4:1093.
[27] Xu Y, Assano T, Kseshuvhi A, Rieck U, Petermann J. J Mater Sci Lett 1989;8:65.
[28] Gan Z, Abe H, Doi Y. Macromol Chem Phys 2002;203:2369.
[29] Schumacher M, Lovinger AJ, Agarwal P, Wittmann JC, Lotz B. Macromolecules 1994;27:6956.
[30] Petermann J, Xu Y, Loos J, Yang D. Polym Commun 1992;33:1096.
[31] Petermann J, Xu Y. Polym Commun 1990;31:428.
[32] Wittmann JC, Lotz B. J Polym Sci, Polym Phys Ed 1985;23:205.